

Dipole measurements for the A0 Photoinjector

Marcellus E. Parker

Summer Internship in Science and Technology

Fermi National Laboratory

Morehouse College

8/7/2009



Advisor: James Santucci

Division: Accelerator Division

Abstract:

The Emittance Exchange (EEX) Project, a Research and Development project at Fermilab focuses on the comparison of transverse to longitudinal emittance exchange is currently ongoing at the A0 Photoinjector. EEX Exchanges longitudinal beam emittance for transverse using dogleg dipole magnets and a TM110 RF cavity. Previous studies at the A0PI have noticed that the electron trajectories through the dogleg dipoles do not follow simulations. It is believed that this discrepancy is due to excessive magnetic fringe fields of the Dog Leg dipoles. Previous measurements of the individual dipole magnets were conducted at the Magnetic Test Facility for currents of 4.5A but not at the 1.8A currently used at the A0PI. This paper describes new measurements and analysis of the dipoles and their fringe fields at 1.8A.

INTRO:

The initial function of the A0 photo- injector was to create an 8nC electron bunch with acceleration to 18MeV. Beam power peak was to reach 16.5MW with 1.3GHz RF[1]. In addition Dipole Chicane magnets were to compress the bunch length to ~ 1 mm. The project was placed into action to comply with the requirements of the TeV Superconducting Linear Accelerator (TESLA). The existing function now is to study beam characteristics and provide a user facility for a 1nC 16MeV electron beam.

Initiating the sequence of the accelerator is a 263 UV laser pulsed at a wavelength of 263nm. Upon interaction with the photo cathode, electron bunches are produced

at several nano Columbs (nC) per bunch. The emittance of the electron bunches are reduced by three Solenoids running at 270A each producing a longitudinal magnetic field of 0.1354T. The RF gun, inside and concentric to the main solenoid, resonates at 1.3GHz and accelerates the electrons from 1eV to 4MeV (see figure 1).

The understood radius of the electron bunch is $\sim 1.2\text{mm}$ with a charge of $Q=0.85\text{nC}$. Upon entering the 9-cell cavity the electrons accelerate from 4MeV to 16MeV. At 16MeV the electrons are sent through a series of quadrapole magnets each with a magnetic field at about 0.2T/m till they are meet with 4 dog leg dipole magnets.

Exerting force in one direction, the TDA magnets send the bunch off at 22.5deg from their original trajectory. Upon entering into the TDA field the direction of the beam is distorted as moving electrons are affected by the dipole or fringe fields between TDA magnets. This paper focuses on the methods taken to map out the fringe field behavior between Dipoles 1 and 2 when they are both energized. It will be for later analysis to determine the cause of beam interruption during the event that the bunch is approaching and is between dipoles 1 and 2. One proposed explanation of this event would be that overlapping fringe fields are distorting the path of travel of the electron bunch. The distance between the two TDA dipole magnets is 869.47mm. Measurements within the fringe fields were taken to obtain visual aid of the behavior of the field lines. The mapped fringe field should suffice as

a means to explain beam behavior between TDA magnets.

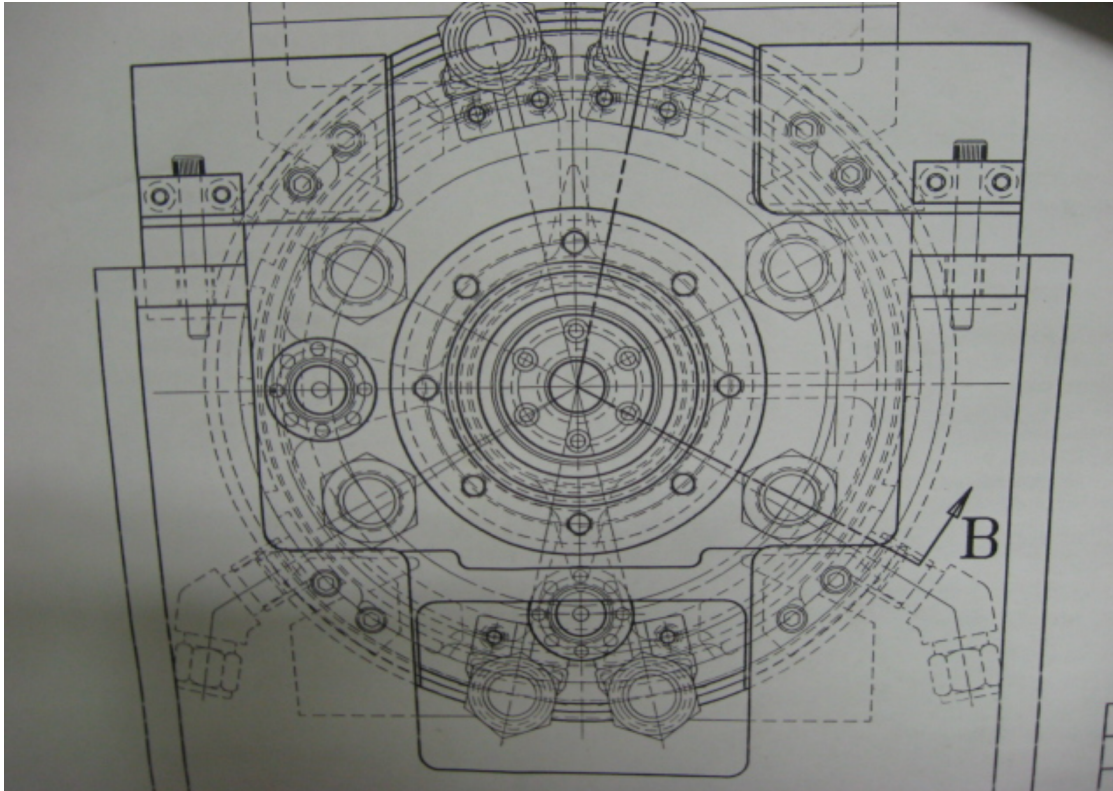


Figure 1.1 Above is a technical drawing of the inside of the first solenoid containing the photocathode and RF Cavity accelerating from 1MeV to 4MeV.

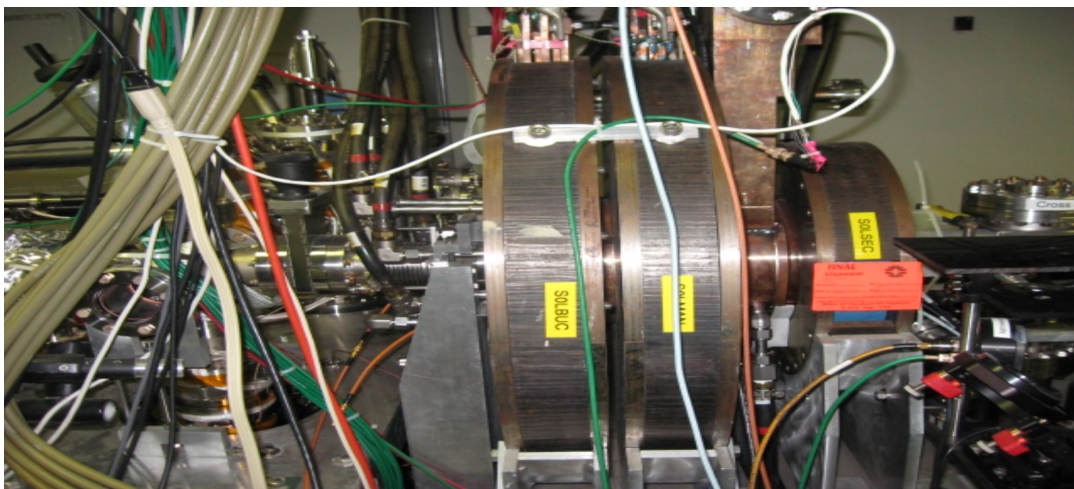


Figure 1.2 below is a side view of the cathode, RF cavity, and three solenoids that lower the emittance to allow the beam to travel downstream.

Initial Observation of Magnetic Flux Density

To form a basis of knowledge surrounding the properties of magnetic flux lines, small-scale measurements were performed on small dipoles. A Quadrupole magnet was rewired to become a dipole magnet thereby making the magnet conduct electricity on two opposite sides with current flowing in the same direction in order to produce a dipole field (see figure 2.1). The magnets were placed on an optics table to conduct measurements. Optomechanics materials were used to fabricate a stand to hold and move the probe horizontally, longitudinally, and vertically.

Forming the magnet is 200 turns of copper wire held in place by soft steel with a permeability of 875×10^{-6} and permeability of air 1.256×10^{-6} H/m. A current of 1A was sent through the rewired Quadrupole to produce the dipole magnetic field. Measurements were taken to determine magnetic flux throughout the space between the opposing sides of the magnet. The flux density was only mapped out in incremented areas of .005m. The X Y plane was parallel to the table while, the probe height was defined to be the Z axis and placed at half the height of the magnet's wall.

The traverse probe required that the flat face of the probe be placed so that field lines run normal to the surface of the probe. The Hall Probe works because of a small metallic plate that sits at the end of the probe (concealed) while small current is sent through the plate. When the flux lines pass through the Nicole plate, current bends to one side of the plate forming a potential difference also know as the Hall

Voltage. Hall Voltage is defined as $\Delta V_H = E_H d = v_d B d$ where d represents the width of the conductor, E is the electric field, B is the magnetic field, v represents drift speed and ΔV is the potential difference in the probe (hall voltage). The total flux density would then be $\Phi_B = \Delta V_H (0.4 \text{ mm}^2)$ which is measured by the Tesla meter. Therefore it becomes essential that the probe's face be normal to the field lines in order to receive an accurate reading.

The developed hypothesis for this measurement was that if two magnetic fields were to be placed close enough to each other so that they may overlap, then the flux density should be the sum of field lines from both magnets. This concept is confirmed in principal from the definition of the magnetic field lines. However, the manner in which the field lines sum up is a function of the amount of current according to Ampere's Law:

$$\mathbf{B} \cdot d\mathbf{l} = \mu_0 I_{in}$$

Where \mathbf{B} is the magnetic field $d\mathbf{l}$ is the change in length, μ_0 is the permeability of the material and I_{in} is the Current inside the wire.

It was assumed that if the flux density read by the hall probe is the sum of the magnetic field lines from each magnet, then the flux density should be the same throughout the majority of the measured area. However, what was actually observed was an increase in the density closest to the magnet's walls. Fringe fields were observed as the probe measured areas near the corners of the magnet.

According to the results from measurements, the flux density was greatest towards the walls of the magnet(see figure 2.1).

According to the figur2.1, the field increased in flux density closest to the sides and decreased towards the center and edges. It is assumed that the edges drop in density as a result of fringe field caused by the geometry of the electromagnet.

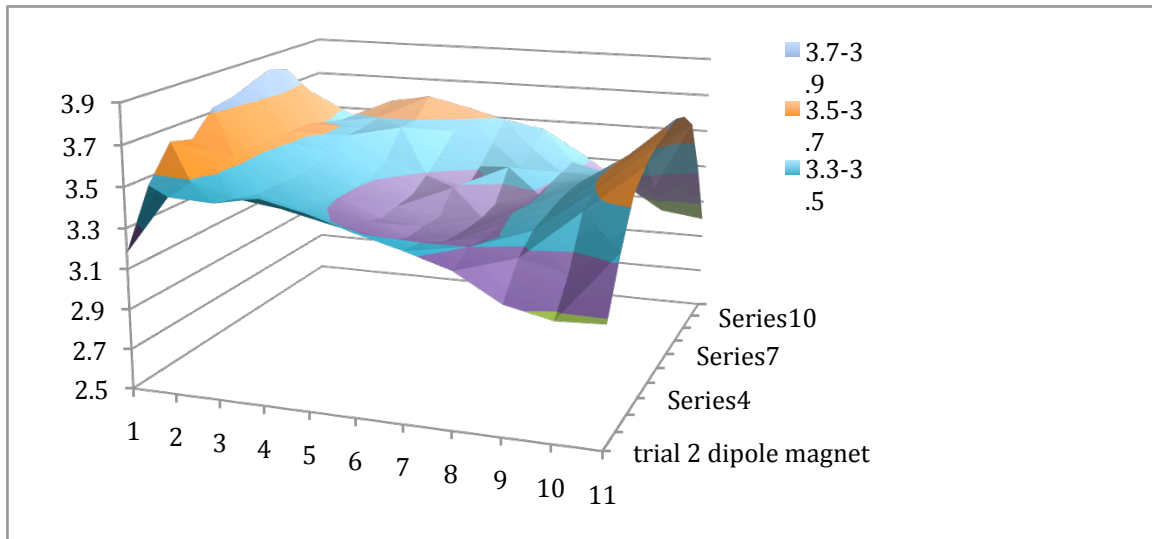


Figure 2.1 above is a plot of the magnetic field within the distance between the two energized sides of the Quadrupole magnet.

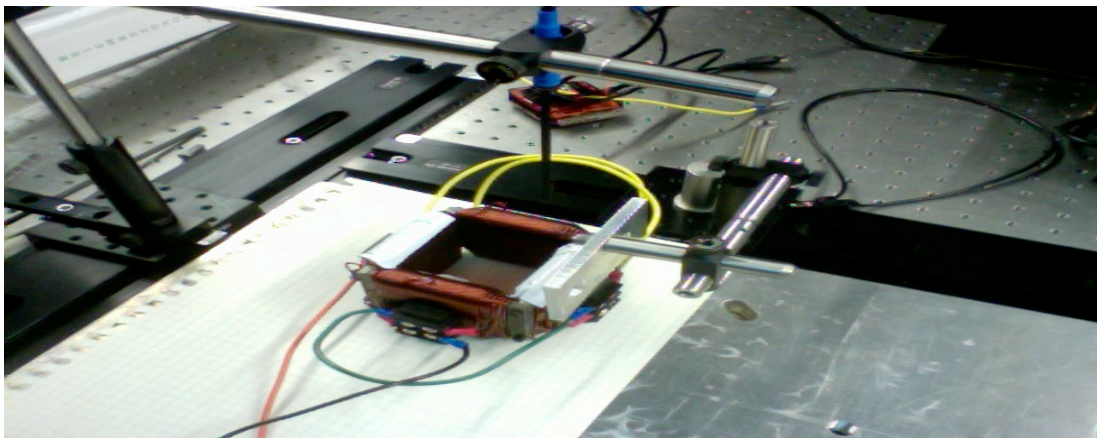
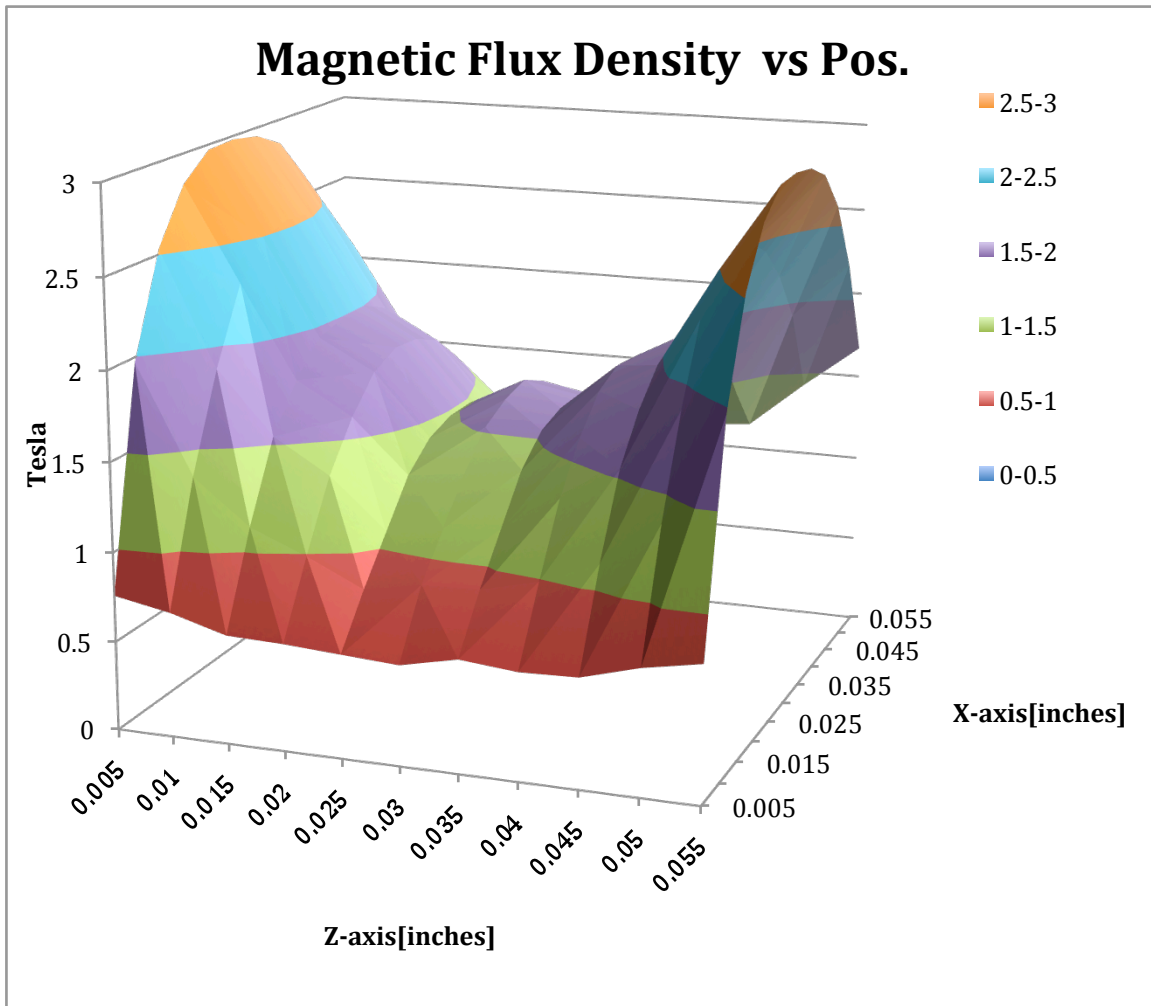
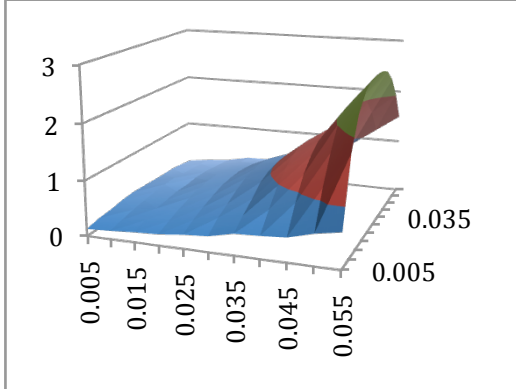
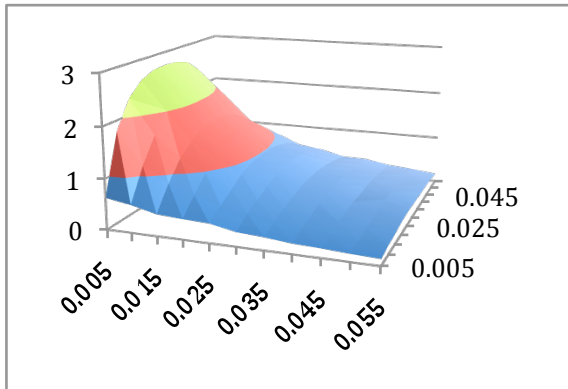


Figure 4.2 displayed above is the transverse probe held up by the fabricated stand taking a reading of the magnetic field



About TDA Magnets

Designed with the purpose of dispersion and compression for emittance exchanges [3], TDA magnets are C framed dipole electro magnets. In the A0 Photoinjector, TDA magnets are designed with two types of geometry's defining the pole tips, Parallelogram and Trapezoidal. The two geometries of pole tips are utilized to reduce quadrupole, sextupole and other possible magnetic field focusing effects of higher orders. Within the A0 Photoinjector laboratory, the magnets are in a "dogleg" set-up (see Figure 3.1) for the purpose of compressing the beam. The desired angle is calculated according to how the beam crosses an imaginary plane leading to the magnetic path of which Lorentz forces interact with the electron bunch. Each of the two magnets were fabricated to have 18 layers of coils wrapped longitudinally around steel 87 times. For purposes of calculating the magnetic, field there are in essence 1,566 turns¹ and a 53mm gap between the pole tips. This produces a magnetic field of $\sim .05\text{T}$ bending the bunch 22.5° . A Beam Position Monitor (BPM) is mounted between each pair of magnets in the beam line for confirmation of the beams position in the Photoinjector. In addition to knowing the beams position, further calculation by done through modeling the dipole field to that of a thin lens to calculate the final position and direction given the initial position, momentum incident angle and momentum of the electron bunch. This formula is derived from Hills differential equation.

¹ Despite the difference in radii of each coil in the 18 different layers it can be assumed that all the flux lines produced from the solenoid will be absorbed into the steel and the distance in which the flux lines traveled to reach the steel will not be of any factor contributing or deducting from the flux density within the steel of the magnet .

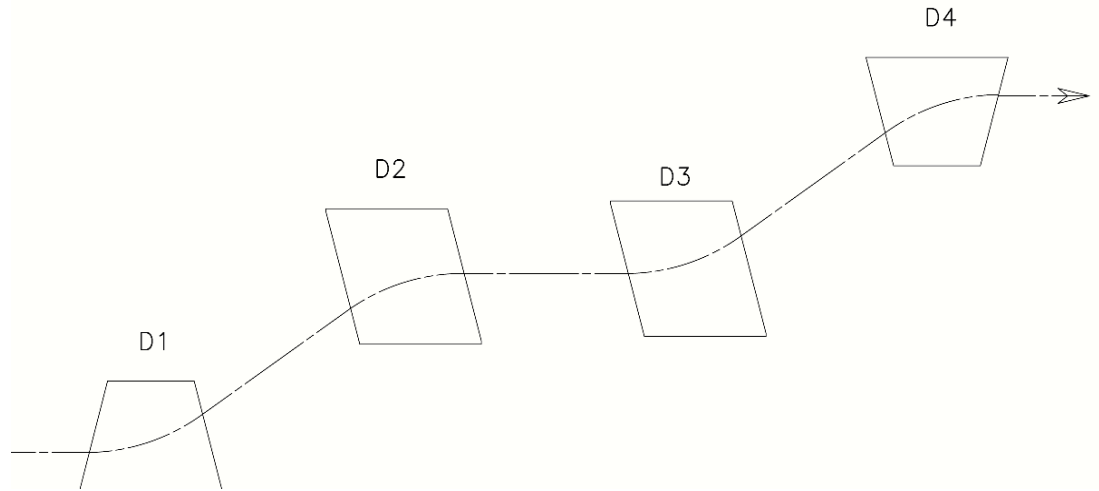


Figure 3.1 Top view of Pole tips arranged in as a double dog leg. The first dog leg spans from D1 to D2 and the second from D3 to D4.

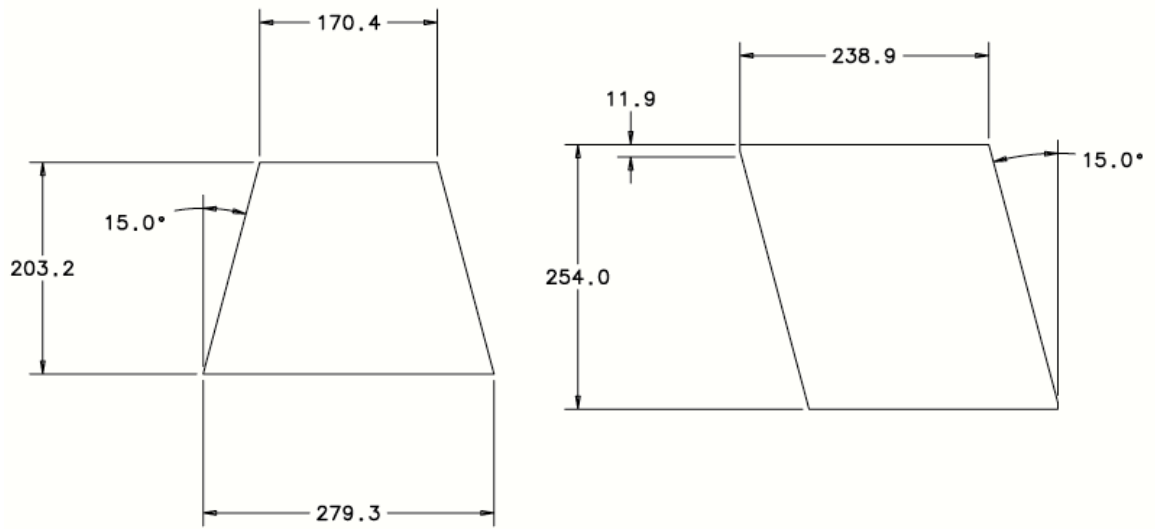


Figure 3.2 dimensions of Trapezoidal and parallelogram pole tips

Beam Optics

Beam optics presents a coherent manner of explaining how an electron bunch can be guided by magnetic forces. The force a charged particle experiences while traveling inside of a magnetic field is expressed through the Lorentz force law:

$$d\mathbf{p}/dt = q (\mathbf{E} + \mathbf{v} \times \mathbf{B}) \quad (3.1)$$

where \mathbf{p} is the momentum t is time, q is the charge, \mathbf{E} the electric field, \mathbf{v} the velocity and \mathbf{B} the magnetic field. This explains the relationship between a charged particle and the magnetic force.

However to explain the behavior of a charged particle in the magnetic field of a dipole magnet, beam optics can be administered to model the magnetic field. Using Hills equation*:

$$u'' + K(s)u = 0 \quad 3.2$$

this equation is a second order differential equation that lacks a first derivative term implying that no dissipating or driving force is encountered. This means that when the bunch is sent through the dipole field there is no loss or gain in energy only a change in direction. Hill equation for purposes of beam optics has been manipulated into a matrix equation to be user friendly.

$$\begin{pmatrix} u \\ u' \end{pmatrix} = \begin{pmatrix} R_{11} & R_{12} \\ R_{21} & R_{22} \end{pmatrix} \begin{pmatrix} u_0 \\ u'_0 \end{pmatrix} \quad (3.3)$$

Where u and u_0 is the final and initial positions, u' and u'_0 is the final and initial angle the particle comes in contact with the magnetic field.

$$\begin{pmatrix} R_{11} & R_{12} \\ R_{21} & R_{22} \end{pmatrix}$$

* This law holds true assuming that no higher or lower order magnetic field affects are present or any energy is lost through radiation.

above is a transformation matrix that is used in optics to express the change in direction in one dimension of the transmitted ray into the direction of the incident ray. For purposes of beam line optics this same matrix equation is used to transform the initial position the beam travels while in the dipole field into the output direction and position of the beam. The entries of the transformation matrix are a function of the bending radius and the bending angle:

$$R = \begin{pmatrix} \cos\theta & \rho\sin\theta \\ -\frac{\sin\theta}{\rho} & \cos\theta \end{pmatrix} \quad (3.5)$$

Where $\rho = p/qB_y$ is the bending radius of the reference particle which for this particular case is the electron bunch. P is the momentum of an electron, q is the charge, and B is the magnetic field produced by the magnet. Determining the matrix for a dipole in three dimensions is a bit more complex:

$$\begin{pmatrix} x \\ x' \\ y \\ y' \\ z' \\ \frac{\Delta p}{p} \end{pmatrix} = \begin{pmatrix} R_{11} & R_{12} & R_{13} & R_{14} & R_{15} & R_{16} \\ R_{21} & R_{22} & R_{23} & R_{24} & R_{25} & R_{26} \\ R_{31} & R_{32} & R_{33} & R_{34} & R_{35} & R_{36} \\ R_{41} & R_{42} & R_{43} & R_{44} & R_{45} & R_{46} \\ R_{51} & R_{52} & R_{53} & R_{54} & R_{55} & R_{56} \\ R_{61} & R_{62} & R_{63} & R_{64} & R_{65} & R_{66} \end{pmatrix} \begin{pmatrix} x_0 \\ x'_0 \\ y_0 \\ y'_0 \\ z'_0 \\ \frac{\Delta p}{p} \end{pmatrix} \quad (3.6)$$

For this matrix x_0 and y_0 x and y are the final positions on the x axis and ,
These transformation matrices are sometimes referred to as Jacobian matrices or “R” matrices.

Beam Compression.

The intended purpose of the TDA magnet is to compress an electron bunch. Dispersion and Compression depends on how the magnets are spaced and positioned in relation to each other. Consider a cloud of electrons all having been accelerated by an RF wave, it can be assumed that the cloud of electron has a higher energy towards the head and lower energy towards the tail. The cloud of electrons also referred to as a bunch is about to travel through a magnetic dog-leg set up. This set up can be seen in figure 3.3 . Upon reaching the dipole field, electrons moving at higher energies spend less time within the magnetic field and travels a shorter path than do electrons traveling at a lesser momentum.

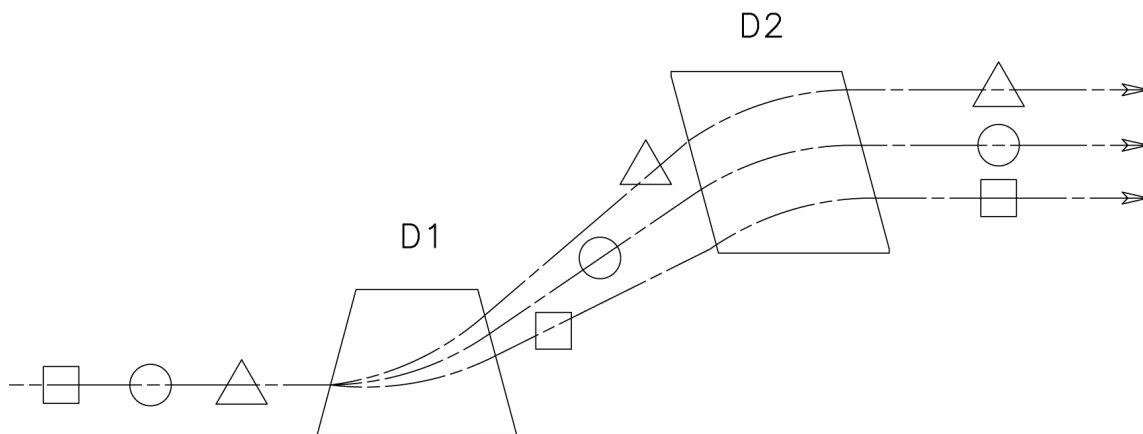


Figure 3.3

Figure 3.2: displayed is a conceptual drawing of the dog leg set up and the path the electron bunch travels when affected by the dipole field. Assuming the head of the bunch (triangle) has less momentum than the tail (square) the head should spend more time travel a longer distance within the magnetic field. There fore we should also see a greater bend in electrons of a lesser momentum compared to electrons of a higher momentum.

TAKING DIPOLE MEASUREMENTS

A change in beam behavior was noticed from previous emittance exchange experiments (see figure 4.1) involving the bunch to travel through the dipole fields. It was noted from the use of a Beam Position Monitor (BPM) that fringe fields produced between dipoles 1 and 2 (refer back to figure 3.1) are causing deformations in the shape of the beam and altering position. As noted by Tim Koeth in his dissertation [3] “corrections to dipole 1 were needed in order to keep the beam horizontally positioned at BPM24 after dipole 2 was energized.” From this observation magnetic measurements appeared to be the logical choice for determining the behavior of fringe fields between the two magnets. Since the particles’ position in space is what is being affected, measurements took place to replicate the field between dipoles 1 and 2.

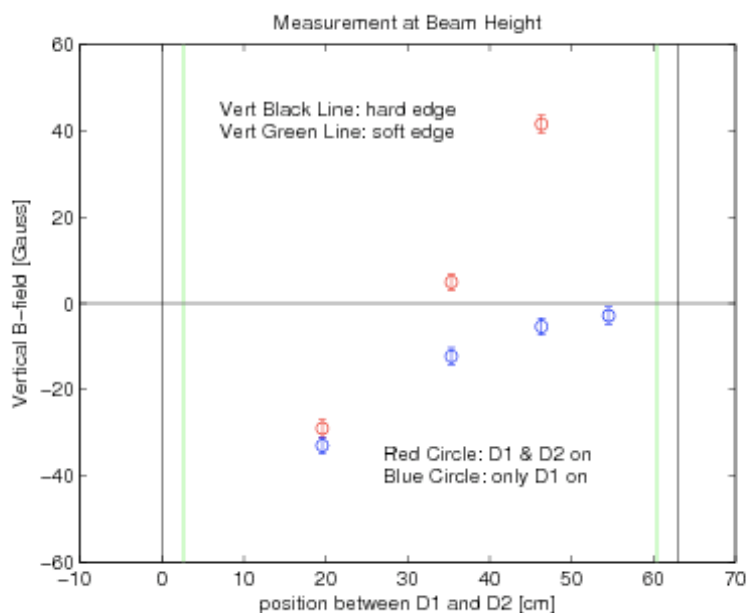


Table 4.1 Above is a measurement of the vertical magnetic field of dipoles 1 and 2

At the A0 south entrance, dipoles of the same shape and geometry's as those in the Photoinjector (see figure 4.2) were lifted by crane to be placed in a truck for transport to the MTF. Once At the MTF the dipoles were then lifted again by crane and brought over to stand B. Since it is particularly necessary to replicate the fringe field interaction between dipole 1 and 2 to understand how the magnets interact with one another, it was necessary to make extensive and precise fringe field measurements. The intended arrangement of the magnets on the stand was to mirror how they are currently placed in the Photoinjector. Three aluminum rectangular shaped blocks were used to provide an elevated surface on which to place the dipoles. The height increase allowed for a minimum of a 2ft distance from any highly permeable materials that may interact with the fringe field. A Brunson scope, accurate to within ($<.001''$), was used to confirm that the magnets were level and parallel to each other just like they are in the Photoinjector.

Once in place it was confirmed that the lateral distance between the two magnets was 51.979mm (2.046') and the longitudinal distance was 508.264mm(20.010") according to the schematic in figure 4.5. A steel scale and gage Blocks were used to confirm measurements within an accuracy of $1/64''$ (0.016). Utilizing the level (Wild) scope, the hall probe was leveled transversely (roll) and longitudinally (yaw) to comply with that of the magnets in the Photoinjector.

For this particular procedure the Z axis was defined as the direction that the beam follows (longitudinal direction), the x axis was the horizontal direction and the y axis was defined as the altitude of the beam which remained constant. A 52"x20" area was measured via transverse magnetic probe. Because of the probe could only measure a longitudinal distance of 11" down the Z axis, the Z ranges were broken up into six different overlapping areas see figure 4.4

Measured Bounds Down z axiz	Current measured in [A]	
-26" → -16"	1.8A	4.5A
-18" → -8"	1.8A	4.5A
-10 "→ 0"	1.8A	4.5A
0 "→ 10"	1.8A	4.5A
8 "→ 18 "	1.8A	4.5A
16" → 26"	1.8A	4.5A

Table 4.3 Displayed is a table of the different overlapping Z ranges

Once in place, the transverse probe was able to conduct measurements on its own. The probe was mounted onto a machine the accurately moves the probe down the Z and X axis according to how it was programmed to function by the computer connected to the probe. For accuracy in each magnetic reading the probe paused for five seconds giving the tip of the tip of the probe time to stop vibrating once the machine has stopped for a reading. Once the magnetic field is recorded by the probe

the information is immediately stored on the computer, thus eventually stored in the online database.

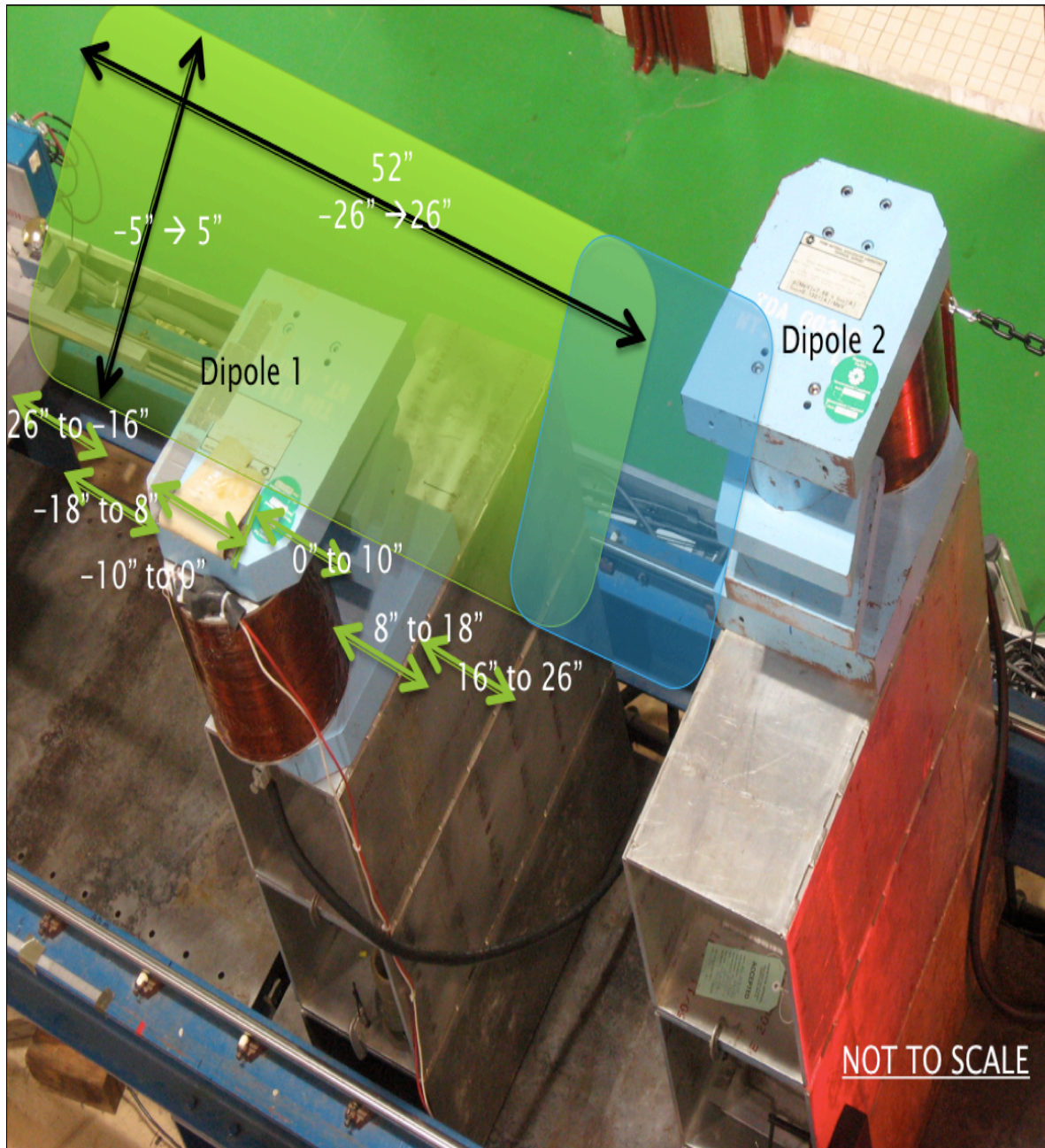


Table 4.4 displays dipoles 1 and 2 on the stand at the magnet test facility. The green region is the complete area measured using a transverse hall probe. The blue region nearest to the second dipole represents the area of the second dipole magnet.

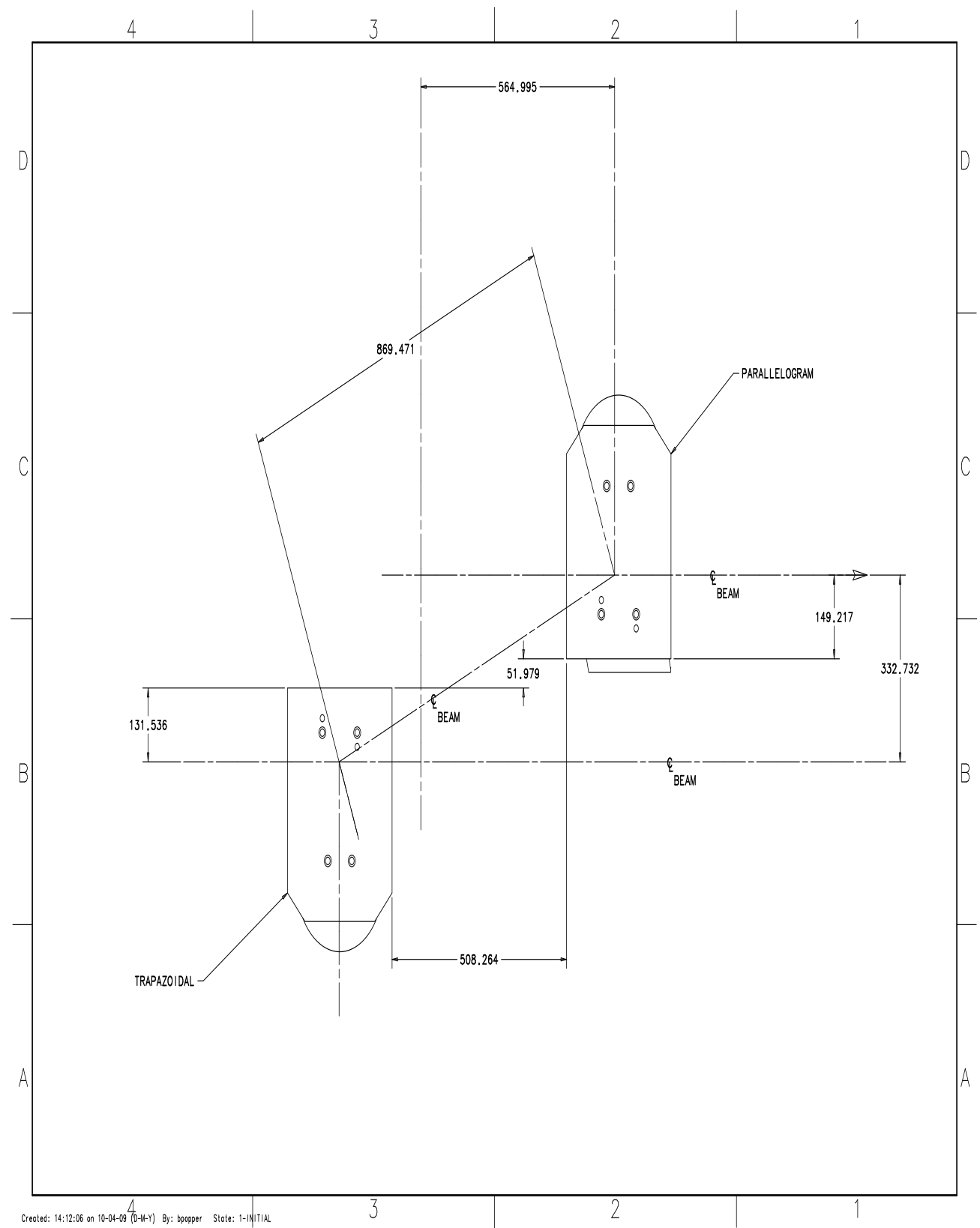


Figure 4.5 Displayed is a schematic of how the magnets were placed at the MTF and their current positioning along the beam line in the Photoinjector

Results

Measurements of the magnets are to confirm or deny the existence of magnetic fringe field between the dipoles. Data obtained from measurements at the MTF was immediately stored in an online data base. All information was analyzed using Microsoft Excel and MATLAB computer code. Excel served the purpose of transferring the data online onto my computer. Data from Excel was copied and pasted into MATLAB code to generate a surface plot for each of the measurements.

Displayed in figure 5.1 is a surface plot of the first dipole magnet energized at 1.8A so that no interaction between the 1st and second dipole can be observed. According to the plot it appears that the surrounding field around the magnet is very low producing a magnetic field of only about $.0 \times 10^9$ [T]. The first measurement of dipole one thus displays no unexpected fringe field behavior leaving the next set of measurements to be suspected of possessing information.

Data from the second set of measurements (when dipole 1 and 2 were energized) was processed in the same manner the first (when dipole 1 was energized) set of measurements. MATLAB provided a clear representation of the fringe field behavior surrounding the first and second dipoles. According to graphed results from the measurements of both dipoles energized at 1.8A, firing field interaction was displayed see figure 5.2. This interaction of fringe field confirms the notion that the first and second dipoles were the probable reasons for why the beam does not follow its expected path of trajectory when traveling in the dog leg arrangement. A difference plot (see figure 5.3) provides a more clear display of the fringe field as the first and second measurements were subtracted from each other

to leave only a plot of the fringe field. The data obtained from measurements at 4.5A produced the same surface plots although at higher magnitudes thus making the observations made at 1.8A plausible for 4.5A.

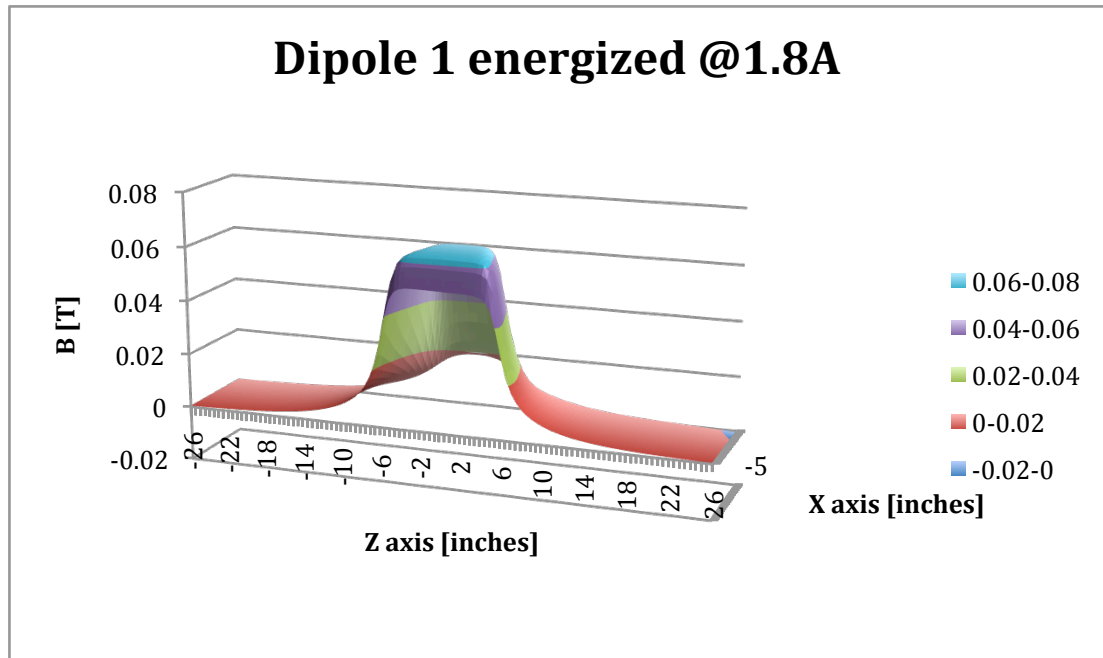


Figure 5.1a Excel plot of dipole 1

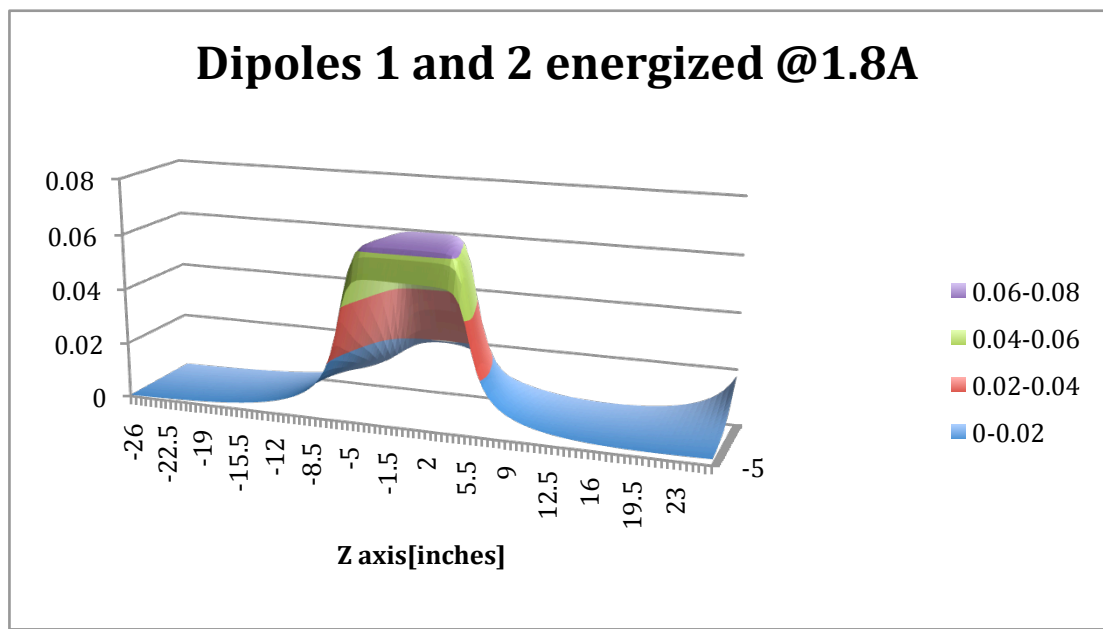


Figure 5.2a Excel plot of dipoles 1 and 2

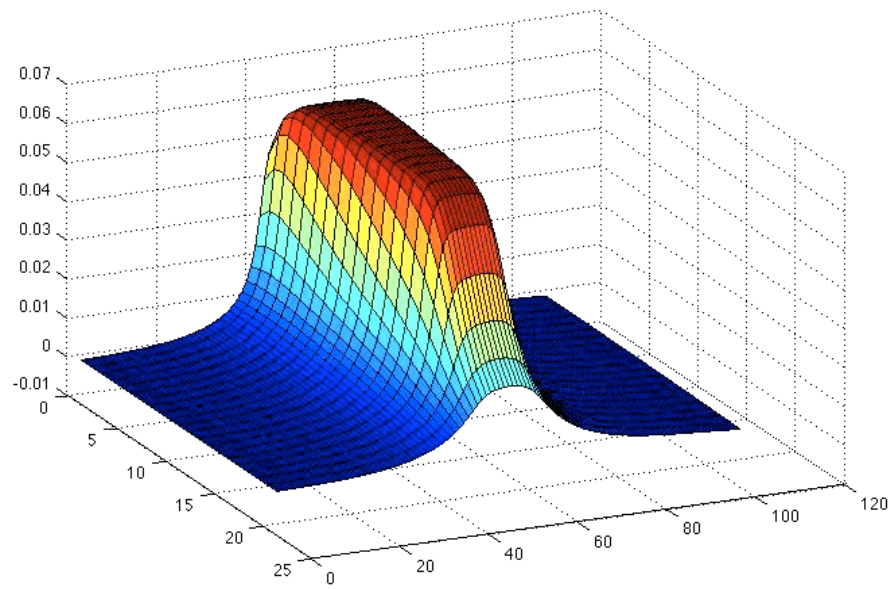


Figure 5.1 MATLAB surface plot of dipole 1 energized at 1.8A

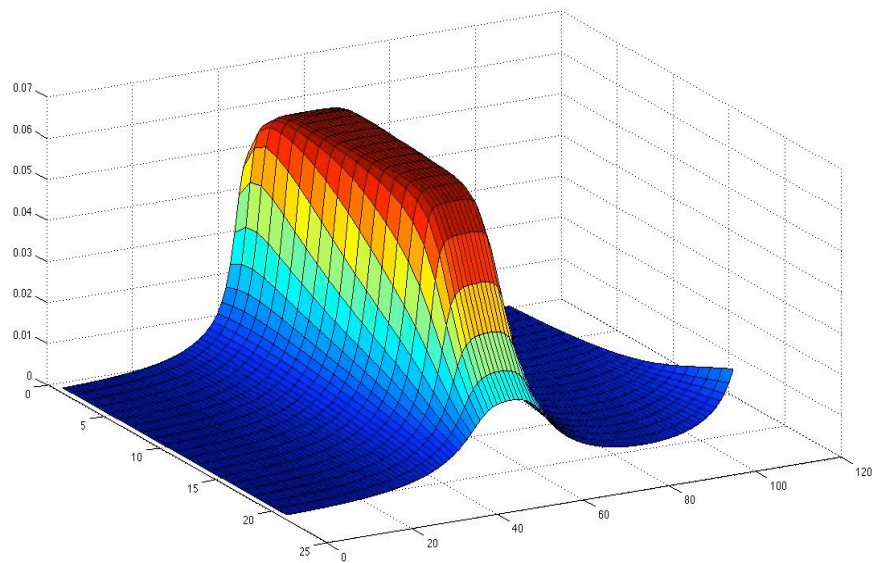


Figure 5.2 MATLAB surface plot of dipoles 1 and 2 energized at 1.8A

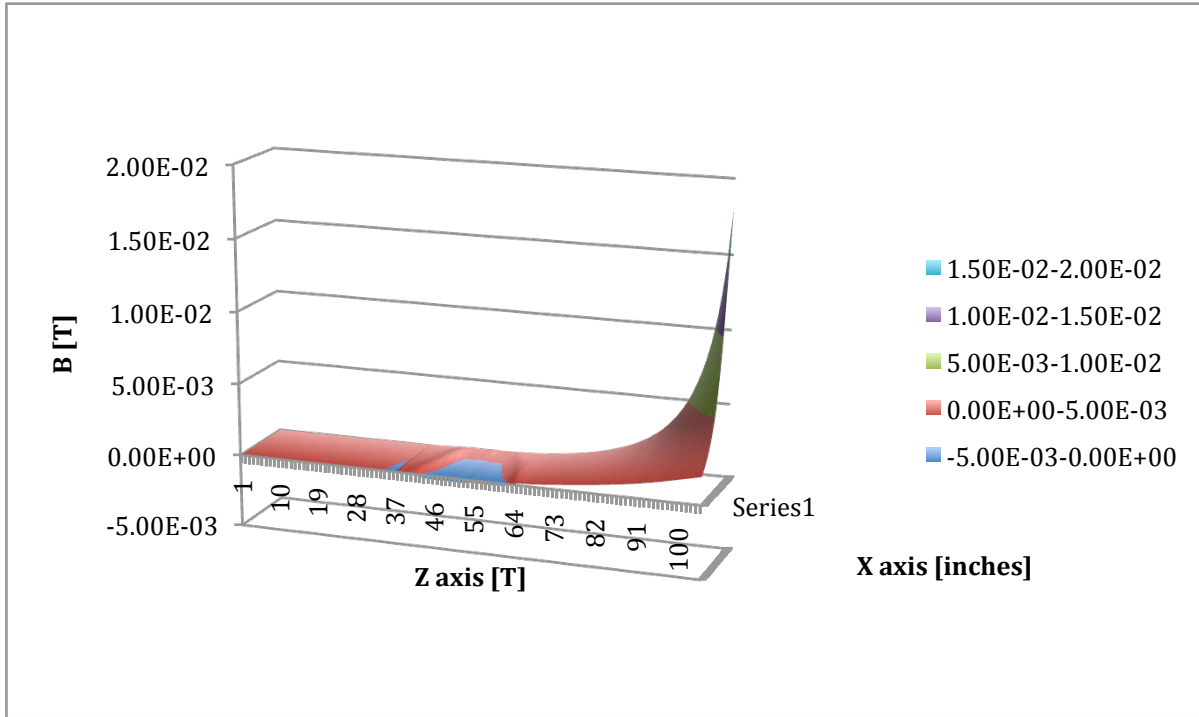


Figure 52.3a Excel surface plot of difference of figures 5.1 and 5.2 isolating fringe field behavior.

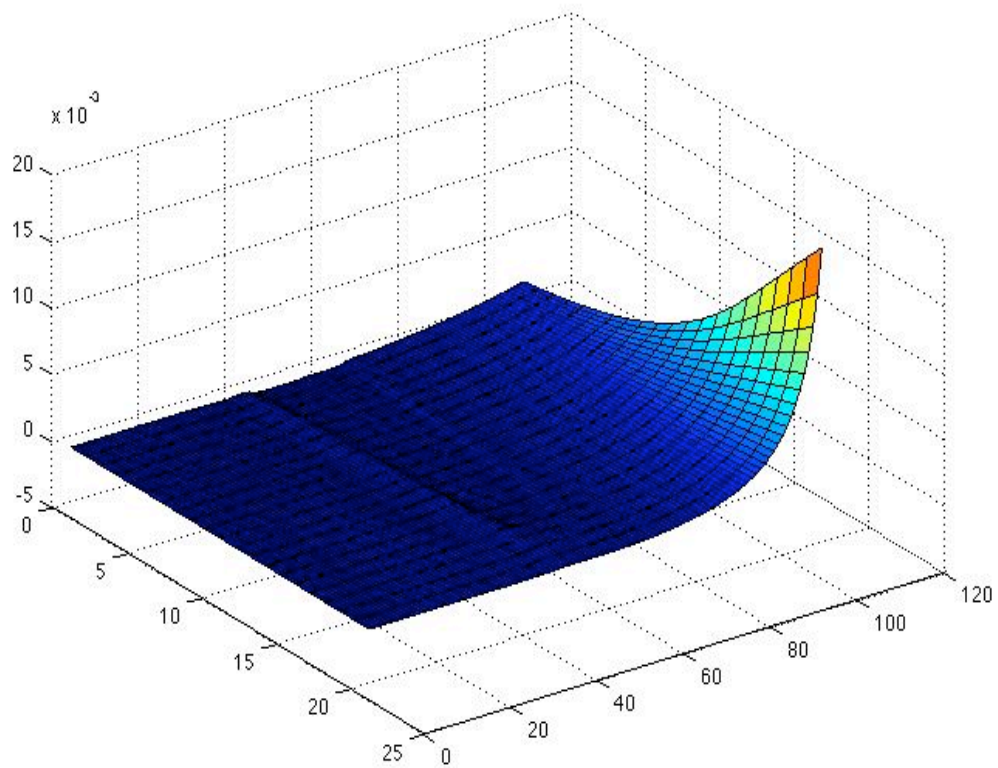


Figure 5.3b Surface plot of difference between figures 5.1 and 5.2

Conclusion

As hypothesized fringe field interaction between dipoles 1 and 2 was observed in the results. In support of the results obtained many precautions were taken to ensure that no variable affected the measurements. Precision equipment confirmed that the magnets were arranged according to their placement in the beam line. Dipoles 1 and 2 were also placed at a distance of two feet away from any ferrous materials that may interact with the fringe field. The experiment, however, was not completely lacking of error sources.

Possible sources of error may have come from a variety of small events. An almost unavoidable error source would be the earth's magnetic field which can sometime be zeroed out during probe calibration. The location in where the measurements took place may have also been a contributing factor. The test stand was not in a closed environment but rather an open facility containing people and other magnetic test that could have contributed small fringe fields to interact with the measurements. Possibly the biggest error source was that the base component of the probe had to be moved after every 11 inches by human hands which could offset measurements by a factor of -0.5cm to 0.5cm. Although, the data appears to be consistent and continuous thereby giving credibility to the accuracy of the obtained data

Now faced with the task of correcting for the interacting fringe fields it may be possible to utilize magnetic shielding. One cost efficient solution would be to create a Mu Metal wall. Mu Metal would be a prime material for such a task because

the permeability if this particular material is high, implying the material is capable of absorbing a high concentration of magnetic field before oversaturation occurs. Another approach would be to invest in the box frame magnet shown in the diagram below, capable of retaining the a higher majority of the fringe field. The demise of this particular approach would be that more costly and not completely reliable.

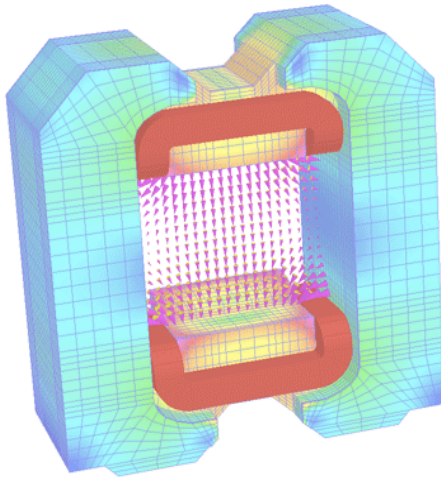


Figure 6.1 Diagram of Box frame magnet.